ORIGINAL PAPER

Electrochemical behavior of aluminum and some of its alloys in chloroaluminate ionic liquids: electrolytic extraction and electrorefining

Sherif Zein El Abedin

Abstract The electrochemical behaviors of pure Al, Al–6%Si, Al–3%Cu, and Al–3.7%Cu–0.9%Mg–0.8%Pb–0.6%Fe alloys were investigated in the chloroaluminate ionic liquids 1-butyl-3-methylimidazolium chloride [BMIm]Cl/AlCl$_3$ (40/60 mol%) and 1-ethyl-3-methylimidazolium chloride [EMIm]Cl/AlCl$_3$ (40/60 mol%). Electrolytic extraction of copper from Al–Cu alloys in the employed ionic liquids was explored. The alloys were anodically dissolved in the ionic liquids and then pure copper was recovered under potentiostatic conditions. Due to the large difference between the deposition potentials of Cu and Al, pure Cu can be obtained without Al contamination. Electrorefining of Al–3%Cu and Al–6%Si alloys was also investigated in [BMIm]Cl/AlCl$_3$ (40/60 mol%) at room temperature. High purity aluminum deposits were obtained with significantly low energy consumption of about 2 kWh/kg of Al.

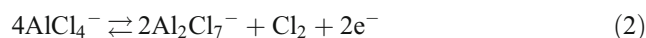## Introduction

Chloroaluminate ionic liquids have been demonstrated to be potential electrolytes for deposition, refining, and recycling

S. Zein El Abedin (✉)
Electrochemistry and Corrosion Laboratory,
National Research Centre,
Dokki,
Cairo, Egypt
e-mail: sherif.zein@tu-clausthal.de

S. Zein El Abedin
Institute of Particle Technology,
Clausthal University of Technology,
Arnold Sommerfeld Str. 6,
38678 Clausthal-Zellerfeld, Germany

of aluminum. As chloroaluminate ionic liquids are non-volatile up to about 120–140 °C, they are regarded as good electrolytes for aluminum deposition and recycling. Numerous studies have been reported on the electrodeposition of Al and its alloys in chloroaluminate ionic liquids; see [1–12]. Although, these liquids allow depositing Al in high quality, a commercial process has not yet been established. Reddy et al. [13, 14] have reported electrorefining of aluminum alloys in chloroaluminate ionic liquids. They have shown that high purity aluminum deposits could be obtained with low energy consumption and no emission of pollutants. Recycling of aluminum metal matrix composite via electrorefining in chloroaluminate ionic liquids at a temperature of 103 °C has been stated [15].

Chloroaluminate ionic liquids are mixtures of anhydrous aluminum chloride and organic halides (RX), like 1-ethyl-3-methylimidazolium chloride, 1-butyl-3-methylimidazolium chloride, and tetraalkylammonium halides. They possess a number of attractive physical properties such as good ionic conductivity, low vapor pressure, good thermal and chemical stability, and good solubility for many inorganic compounds [16–18]. Furthermore, they show adjustable Lewis acidity over a wide range of AlCl$_3$/RX molar ratios [19, 20]. Liquids with more than 50 mol% AlCl$_3$ are Lewis acidic; less than 50 mol%, Lewis basic; and neutral if the molar ratio AlCl$_3$/RX is 1. In acidic liquids with less than 67 mol% AlCl$_3$, AlCl$_4^-$ and Al$_2$Cl$_7^-$ are the dominant anionic species and the liquids are acidic due to the presence of the latter species which is a halide ion acceptor. The electrochemical window of the acidic liquids is limited by the reduction of Al$_2$Cl$_7^-$ and oxidation of AlCl$_4^-$ as follows:

$$4Al_2Cl_7^- + 3e^- \rightleftharpoons Al + 7AlCl_4^- \qquad (1)$$

$$4AlCl_4^- \rightleftharpoons 2Al_2Cl_7^- + Cl_2 + 2e^- \qquad (2)$$

Therefore, electrodeposition of aluminum can be performed in acidic melts by reduction of $Al_2Cl_7^-$, the only reducible aluminum containing species within the electrochemical window of this kind of ionic liquids [21, 22]. In liquids with more than 67 mol% $AlCl_3$, $Al_3Cl_{10}^-$, $Al_4Cl_{13}^-$, and Al_2Cl_6 are present [23]. In basic liquids, $AlCl_4^-$ and Cl^- are the principal constituents, and they are basic due to the presence of chloride ions which are not bound to aluminum. The electrochemical window is limited by the reductive decomposition of the organic cation and the oxidation of Cl^- to chlorine. The neutral liquids exhibit the widest electrochemical window compared with the acidic and basic liquids as the major anionic species is only $AlCl_4^-$, and hence the limits of the electrochemical window are set by reduction of the organic cation and oxidation of $AlCl_4^-$. Low amounts of Cl^- and $Al_2Cl_7^-$ are always present in neutral liquids as a result of the following autosolvolysis reaction [22]:

$$2AlCl_4^- \rightleftarrows Al_2Cl_7^- + Cl^- \qquad (3)$$

In the same way, very small amounts of $Al_2Cl_7^-$ and Cl^- are always present in basic and acidic liquids, respectively [22].

The present work aims at exploring the capability of using chloroaluminate ionic liquids as potential electrolytes for the electrolytic recovery of less reactive metals, especially copper, from aluminum alloys. Two ionic liquids namely, [EMIm]Cl/AlCl₃ (40/60 mol%) and [BMIm]Cl/AlCl₃ (40/60 mol%) were employed in this work. Understanding of the electrochemical behavior of Al–alloys in the employed ionic liquids is an important step for application of ionic liquid electrolytes for recycling and electrorefining of aluminum. It is worth mentioning that the electrochemical behavior of the tested alloys in both liquids is identical. It is demonstrated that pure copper can exclusively be obtained under potentiostatic conditions, after anodic dissolution of Al–Cu alloys in the employed ionic liquids. Furthermore, high purity aluminum can be recovered by electrorefining of aluminum alloys with significantly low energy consumption.

Experimental

[BMIm]Cl/AlCl₃ (40/60 mol%) and [EMIm]Cl/AlCl₃ (40/60 mol%) supplied by BASF were employed in the present study. The color of the liquids was dark brown indicating the presence of impurities. Therefore, the liquids were subject to purification by electrolysis between two Al electrodes for several days in an argon filled glove box with water and oxygen contents below 20 ppm (OMNI-LAB from Vacuum Atmospheres). Such purification procedure can remove the protonic impurities and other impurities (see [24]). After purification, a yellowish liquid was obtained.

All electrochemical measurements were performed in the glove box using a Parstat 2263 Potentiostat/Galvanostat (Princeton Applied Research) controlled by PowerCV and PowerStep software. A 150-ml glass beaker was used as an electrochemical cell with three electrodes. Measurements were made on pure Al (99.999%), Al–6%Si, Al–3%Cu, commercial Al–3.7%Cu–0.9%Mg–0.8%Pb–0.6%Fe alloy and on gold substrates (Arrandee—gold films of 200–300 nm thickness deposited on chromium-covered borosilicate glass). AlCuMgPbFe alloy is commercially available, whereas Al–6%Si and Al–3%Cu alloys were prepared from pure aluminum (99.99%) and high purity silicon and copper, respectively. Aluminum and an appropriate amount of alloying elements were melted in a steel crucible at temperatures between 750 and 800 °C for about 3 h. The alloy melt was then poured into a rectangular steel mold and left to cool in air. The prepared alloys were used in the cast state. Directly before use, the electrodes were abraded successively with emery paper of increasing fineness up to 600, and then degreased with acetone in an ultrasonic bath for about 5 min. The gold substrates were heated in a hydrogen flame to slightly red glow for several minutes. Al wires (99.999%) and Al sheets (99.99%) were used as reference and counter electrodes, respectively. The reference electrode was immersed in the neat ionic liquid and separated from the test electrolyte by a fine porosity frit. The anodic dissolutions of Al–3%Cu and Al–3.7%Cu–0.9%Mg–0.8%Pb–0.6%Fe alloys were carried out using a Teflon cell with a Nafion membrane to separate the working and counter/reference electrodes.

For electrorefining experiments, Al sheets (99.99%) were used as cathodes and the tested alloys as anodes. The working surface areas of the cathode and the anode were 4 cm². The distance between the cathode and the anode was fixed at 2 cm and 100 mL of the employed ionic liquid was used for each experiment. The energy consumed during the electrorefining was estimated using the following equation [15]:

$$E = V(Q/\eta_{eff.})$$

where, V is the applied cell voltage, $\eta_{eff.}$ is the cathode current efficiency, and Q is the theoretical charge required for depositing a definite amount of material according to the Faraday's law. The cathode (anode) current efficiency is the ratio of the actual amount of metal deposited (dissolved) to that expected theoretically.

A scanning electron microscope (CamScan) attached with energy dispersive X-ray analyzer (EDX) was utilized to investigate the surface morphology and the chemical composition of the tested alloys. The precise detection limit of our EDX analyzer is 0.1 wt.%.
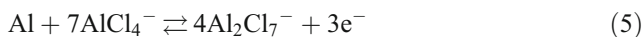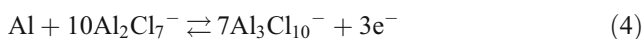
Fig. 1 Cyclic voltammograms recorded on Al in [BMIm]Cl/AlCl$_3$ (40/60 mol%). *Inset* the potential was scanned from the open circuit potential in the positive direction up to 1 V, then scanned back to −0.1 V and terminated at 1 V. The scan rate was 10 mV s^{-1}
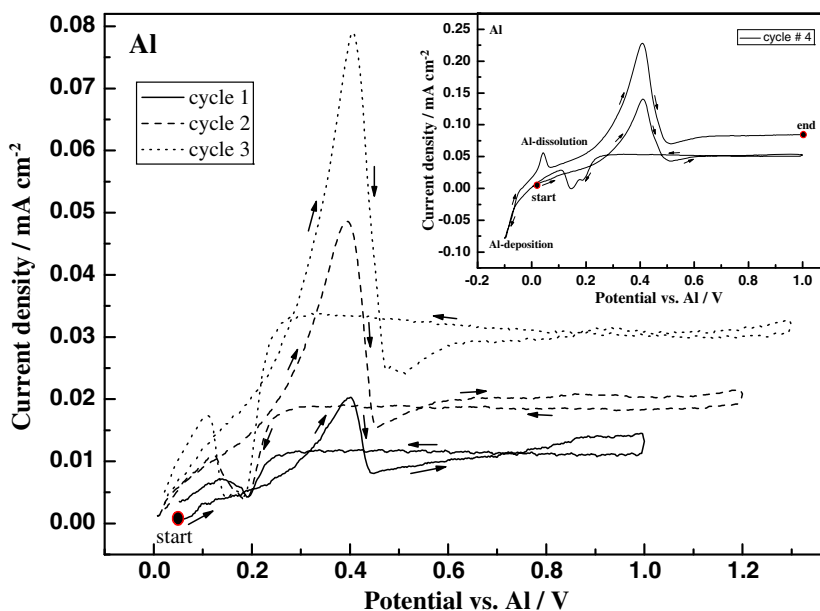
Results and discussion

Electrochemical behavior in [BMIm] Cl/AlCl$_3$ (40/60 mol%)

The cyclic voltammetry behavior of pure aluminum was investigated in the ionic liquid [BMIm]Cl/AlCl$_3$ (40/60 mol %) at room temperature. Figure 1 shows a set of cyclic voltammograms recorded on Al in the employed ionic liquid. The potential was scanned from the open circuit potential in the positive direction up to different potentials, 1, 1.2, 1.3 V (vs. Al) in cycle 1, 2, and 3, respectively, and then scanned back to the initial potential. As shown in Fig. 1, on scanning the potential in the positive direction, the anodic current increases smoothly, reaching a maximum value at a potential of about 0.4 V. Then the current decreases rapidly, attaining a relatively constant value. Taking into account that the employed ionic liquid is a Lewis acidic with a molar concentration of 40/60 mol% [BMIm]Cl/AlCl$_3$, thus the dominant anionic species are Al$_2$Cl$_7^-$ and AlCl$_4^-$. Hence, the increase in the anodic current might be attributable to the dissolution of aluminum by the action of Al$_2$Cl$_7^-$ as reported in ref. [25] and by AlCl$_4^-$ as the following:

$$Al + 10Al_2Cl_7^- \rightleftarrows 7Al_3Cl_{10}^- + 3e^- \qquad (4)$$

$$Al + 7AlCl_4^- \rightleftarrows 4Al_2Cl_7^- + 3e^- \qquad (5)$$

As also very small amounts of Cl$^-$ are present in the acidic liquid, Al might be attacked by Cl$^-$ forming AlCl$_3$ (Al + 3Cl$^- \rightleftarrows$ AlCl$_3$ + 3e$^-$). The continues anodic dissolution of Al requires the formation of soluble Al(III) species as described in Eqs. 4 and 5. However, as a result of the thickening of the diffusion layer of Al$_2$Cl$_7^-$ and AlCl$_4^-$, the anodic current drops until a steady state is reached. A surface film of, for example, AlCl$_3$, Al$_2$Cl$_6$ and/or Al$_3$Cl$_{10}^-$ (as oxidation products) might be formed on the electrode surface. This surface film gives some sort of passivity to the electrode surface. However, the high anodic current reveals that the film is not protective and the electrode might undergo further dissolution. On the reverse scan, the formed film dissolves at a potential of about 0.2 V. By successive potential scans, the anodic current increases due to the increase of the surface roughness as a result of anodic dissolution and subsequent pitting. It was also investigated whether the deposition of Al influences the anodic behavior of the Al electrode in the employed ionic liquid or not, inset of Fig. 1. As seen, after scanning the potential in the negative direction, down to −0.1 V, the cathodic current increases due to deposition of aluminum and a stripping peak is observed on the anodic branch of the cyclic voltammogram. Then the same anodic behavior is obtained. As shown in the inset of Fig. 1, the stripping of the electrodeposited aluminum occurs at a lower potential than the dissolution of Al matrix. This indicates the higher activity of the freshly deposited aluminum.

The examined alloys exhibit cyclic voltammetry behaviors similar to that of pure aluminum (see Figs. 2 and 3). As a conclusion, the voltammetric studies reveal that Al and the examined alloys are subject to anodic dissolution followed by some sort of passivity in the employed ionic liquid. There are several factors that could be attributable to the observed "passivity", or better to say "film formation exerted some kind of passivity": precipitation of AlCl$_3$, Al$_2$Cl$_6$, or Al$_3$Cl$_{10}^-$ during Al oxidation and/or adsorption of monovalent to trivalent Al-intermediates. As in the case

Fig. 2 Cyclic voltammograms recorded on Al–6% Si in [BMIm]Cl/AlCl$_3$ (40/60 mol%). *Inset* the potential was scanned from the open circuit potential in the positive direction up to 1 V, then scanned back to −0.3 V and terminated at 1 V. The scan rate was 10 mV s^{-1}
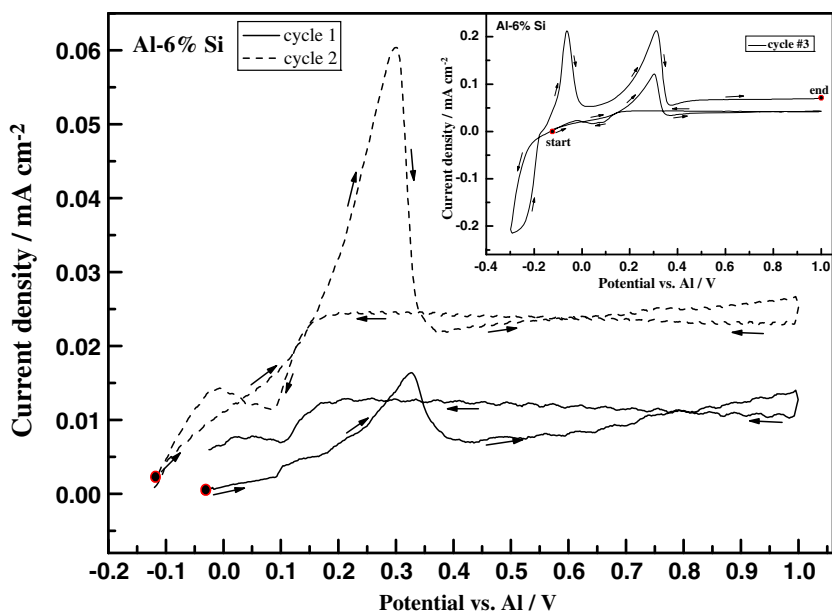
of Al electrode, the stripping of the electrodeposited aluminum on Al–6%Si alloy occurs prior to the oxidation of the alloy surface, inset of Fig. 2.

In the light of the above results, it can be concluded that Al–6%Si and Al–3%Cu alloys can be anodically dissolved in the employed ionic liquid. After applying a current density of 2.4 mA cm^{-2} for 24 h, 0.256 g of Al–3%Cu alloy was dissolved with current efficiency slightly more than 100% (103%). Supposing that the copper was perfectly distributed in the alloy matrix and the alloy homogenously dissolved, the concentration of the copper ions in the electrolyte was estimated to be about 2×10^{-3} mol/L. The observed current efficiency signifies that the alloy

undergoes non-Faradic dissolution, i.e., chemical dissolution, by the action of the employed ionic liquid. How to interpret the slight increase in the current efficiency of the anodic dissolution of the alloy? As the ionic liquid is well purified and all protonic impurities have been removed during the purification process, it is reasonable that some moisture from the glove box reacted with the ionic liquid throughout the duration of the experiment (24 h) librating HCl which chemically attacks the alloy. The visual observation of the anode after the experiment supports the above interpretation as the upper part of the anode—at the interface between the ionic liquid and the inertgas of the glove box—shows higher attack compared with the lower

Fig. 3 Cyclic voltammograms recorded on Al–3%Cu in [BMIm]Cl/AlCl$_3$ (40/60 mol%). *Inset* first cycle. The scan rate was 10 mV s^{-1}
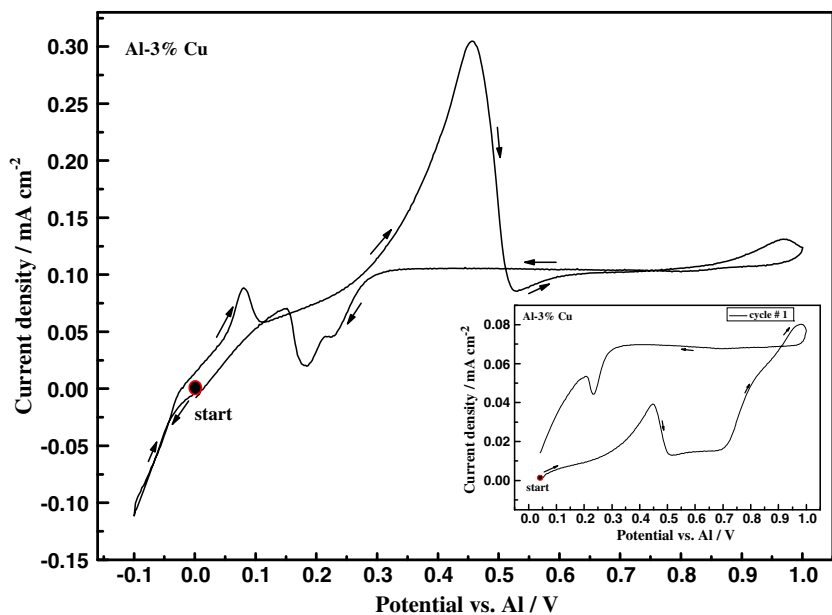
part. It is worth noting that if the experiment was performed for shorter times, the efficiency of the anodic dissolution was found to be close to 100%. Furthermore, the alloy was subject to slight self-corrosion in the employed ionic liquid after an elongated immersion time (more than 24 h). It is reasonable that the existence of copper might enhance the self corrosion of the alloy due to the presence of numerous galvanic sites at the surface. In the next section, it will be shown that copper can be selectively extracted from the ionic liquid containing the dissolution product of Al–3%Cu alloy.

Fig. 4 Cyclic voltammograms recorded on gold in [BMIm]Cl/AlCl$_3$ (40/60 mol%) free and containing the anodic dissolution products of Al–3%Cu alloy at different reversal potentials. The scan rate was 10 mV s^{-1}

Recovery of Cu from [BMIm]Cl/AlCl$_3$ containing the dissolution products of Al-3%Cu alloy

The cyclic voltammetry behaviors of [BMIm]Cl/AlCl$_3$ (40/60 mol%) free and containing the anodic dissolution products of Al–3%Cu alloy were investigated on gold substrates (Fig. 4). The cyclic voltammetry behavior of the neat ionic liquid was studied in order to explore the effect of the anodic dissolution products of the examined alloy on the voltammetry behavior. As shown in Fig. 4a, the cyclic voltammograms exhibit several cathodic processes prior to the bulk deposition of Al. Figure 4b shows these processes with a higher resolution. As manifested, the cyclic voltammogram of the neat ionic liquid shows three cathodic processes (a, b, and c) with the corresponding anodic counterparts (a′, b′, and c′) before the bulk deposition of Al sets in. The cathodic waves (a) and (b) are assigned to different under potential deposition processes (upd) which
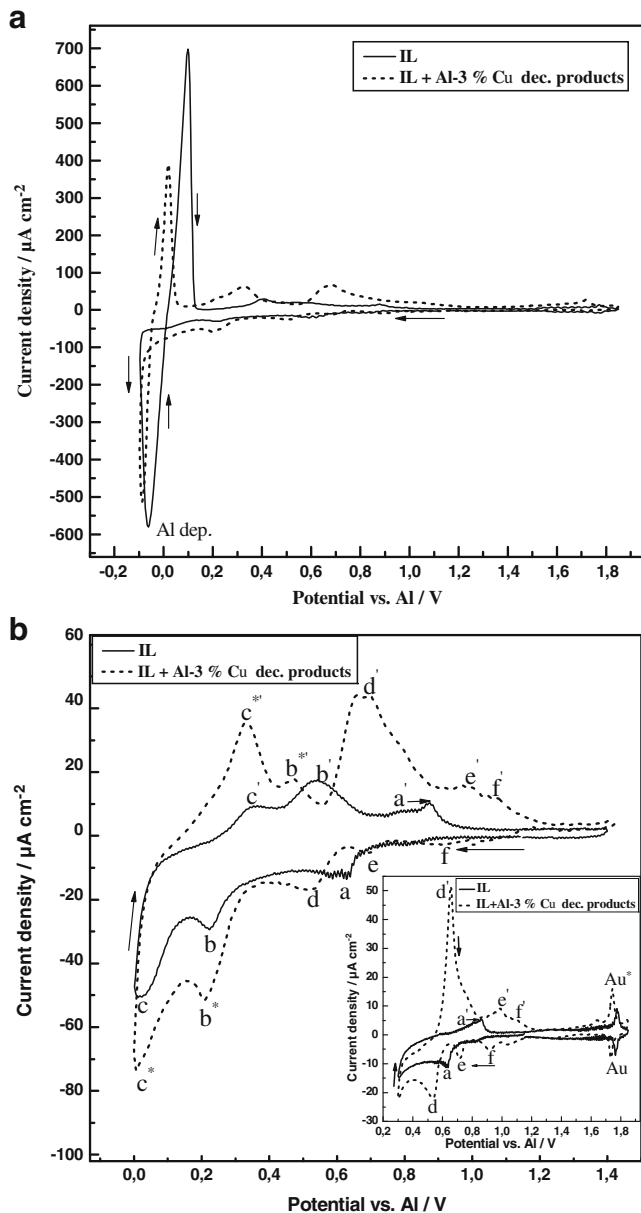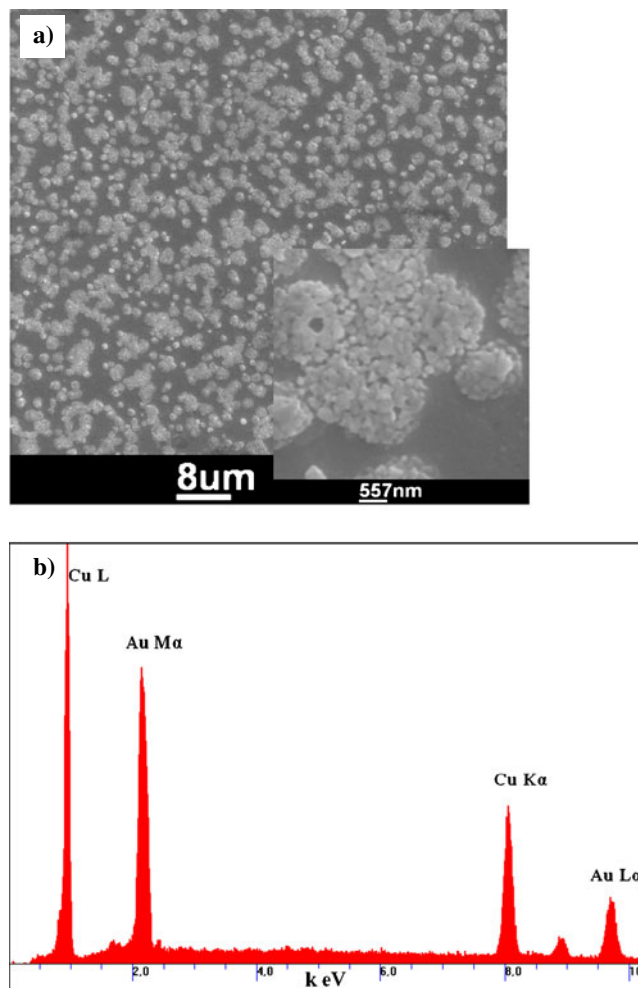

Fig. 5 **a** SEM micrograph of the deposit obtained potentiostatically at a potential of +0.25 V (vs. Al) in [BMIm]Cl/AlCl$_3$ (40/60 mol%) containing the dissolution product of Al–3%Cu alloy. *Inset* SEM micrograph of higher magnification. **b** EDX of the deposit shown in the SEM micrograph
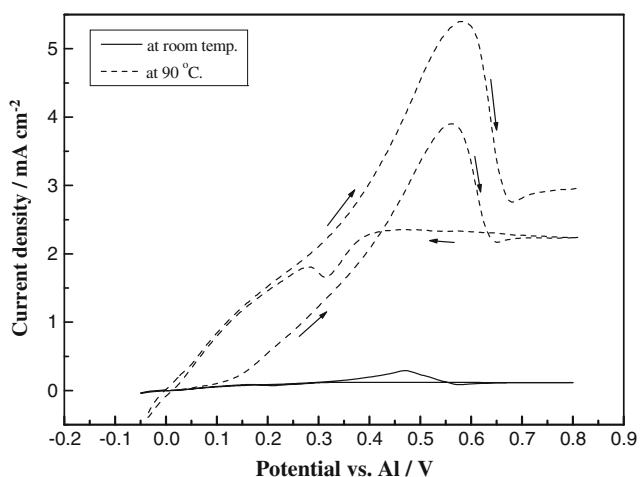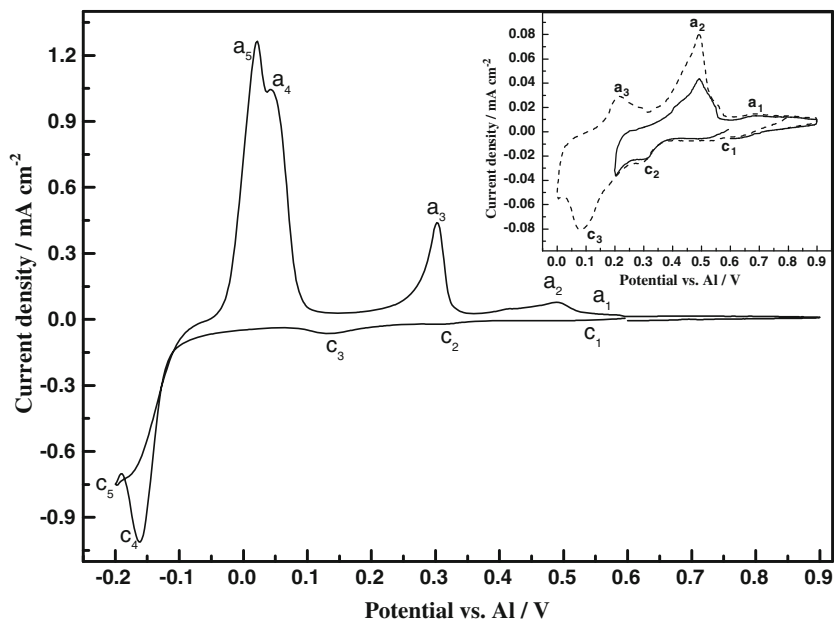
Fig. 6 Cyclic voltammograms recorded on AlCuMgPbFe alloy in [EMIm]Cl/AlCl$_3$ (40/60 mol%) at room temperature and at 90 °C. The scan rate was 10 mV s^{-1}

involve the formation of alloy phases of aluminum on gold as observed using in situ scanning tunneling microscopy, see [26]. The cathodic process (c) observed at about 0 V (vs. Al) is due to the starting of 3D nucleation of aluminum. The cyclic voltammogram of the employed ionic liquid containing the anodic decomposition products of Al–3%Cu alloy exhibits five cathodic processes preceding the bulk deposition of Al. The two redox couples (e/e′) and (f/f′) are correlated to upd processes of Cu on Au. The upd processes are associated with the formation of an alloy phase of Au–Cu and growing of a Cu monolayer [27]. The cathodic process d is corresponding to the bulk deposition of Cu. A pronounced stripping peak of Cu (d′) was recorded on the anodic branch of the cyclic voltammogram. This redox

process was not observed in case of the neat ionic liquid as clearly shown in the inset of Fig. 4b. Furthermore, the reduction processes (b*) and (c*) exhibit higher cathodic currents than those of waves (b) and (c)—which observed in the neat ionic liquid—indicating the contribution of Cu codeposition to both processes. The redox couple Au*/Au obtained at a potential of about +1.75 (vs. Al) is attributable to the gold oxidation/deposition at the step edges of the gold substrate [28]. The bulk oxidation of gold starts at a potential of about +1.95 V (vs. Al). The voltammetry behavior of the ionic liquid containing the anodic decomposition products of the Al–3% Cu alloy reveals that Cu can be potentiostatically recovered at a potential range of 0.5–0.2 V. The scanning electron microscope (SEM) micrographs of Fig. 5a show the surface morphology of a thin Cu layer electrodeposited at a potential of +0.25 V in the ionic liquid electrolyte containing the anodic dissolution products of Al–3%Cu alloy. The deposit contains large agglomerated particles in the order of 1–4 μm in size. These particles consist of small crystallites in the nanometer regime, as shown in the inset of Fig. 5a which shows a higher magnification SEM micrograph. The electrodeposit was analyzed as pure copper as revealed in the accompanied EDX profile of Fig. 5b.

Anodic behavior of AlCuMgPbFe alloy in [EMIm]Cl/AlCl$_3$ (40/60 mol%)

The anodic behavior of the commercial Al–3.7%Cu–0.9% Mg–0.8%Pb–0.6%Fe alloy was investigated in [EMIm]Cl/ AlCl$_3$ (40/60 mol%). Figure 6 shows two cyclic voltammograms of the tested alloy in the employed ionic liquid at room temperature and at 90 °C. The measurements were

Fig. 7 Cyclic voltammograms recorded on gold in [EMIm]Cl/ AlCl$_3$ (40/60 mol%) containing the anodic dissolution products of AlCuMgPbFe alloy. The scan rate was 10 mV s^{-1}. *Inset* CVs at two different reversal potentials

performed at 90 °C in order to show the effect of the increase in temperature on the anodic behavior of the examined alloy. As known, both conductivity and viscosity of the employed ionic liquids improve as the temperature increases. In the cyclic voltammogram recorded at 90 °C, the potential was scanned from the open circuit potential in the positive direction up to a potential of +800 mV (vs. Al), then scanned back to a potential of −50 mV and finally terminated at a potential of +800 mV. The two cyclic voltammograms exhibit the same general feature; however, at 90 °C the current values are about factor 7 higher than the currents recorded at room temperature. This is due to the increased mobility of the electroactive species towards the electrode surface which, in turn, leads to increase the reaction rates. As shown in the CVs, the anodic current increases smoothly reaching a maximum value at a potential of about +550 mV. Then, the current decreases rapidly, reaching a relatively constant value. The increase in the anodic current is due to the anodic dissolution of the

alloy, and then an adsorbed film of the oxidation products might be formed on the electrode surface. This surface film is responsible for the observed constant current. However, the high anodic current reveals that the film is not protective and the electrode might undergo further dissolution. On the reverse scan, the formed film dissolves at a potential of about +300 mV. By successive potential scans, the anodic current increases due to the increase of the surface roughness as a result of anodic dissolution. After applying an anodic current density of 11 mA cm^{-2} at 90 °C for 16.66 h, 0.6 g of the tested alloy was dissolved in the employed ionic liquid. The resulting electrolyte was employed to electrodeposit Cu.

Recovery of Cu from [EMIm]Cl/AlCl$_3$ containing the dissolution products of AlCuMgPbFe alloy

Figure 7 shows the cyclic voltammetry behavior of [EMIm]Cl/AlCl$_3$ (40/60 mol%) containing the dissolution products
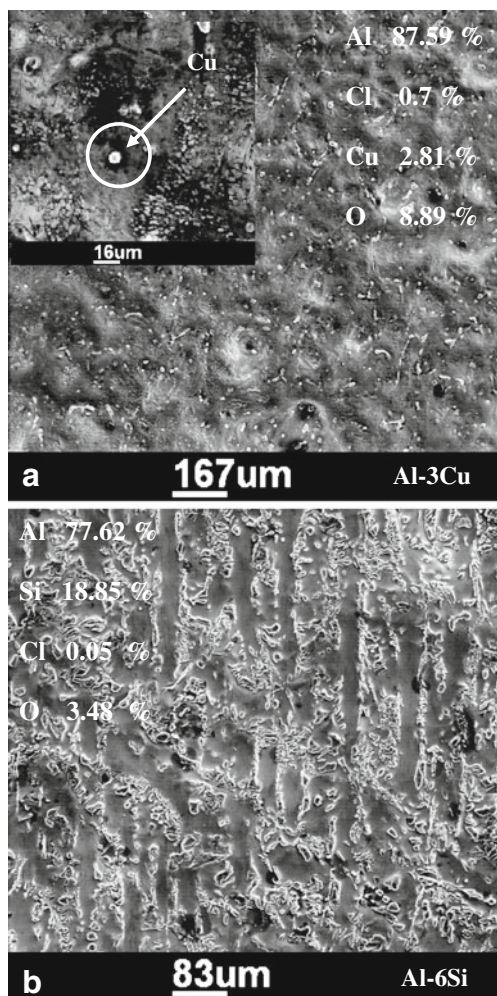

Fig. 8 SEM micrographs of **a** Al–3%Cu and **b** Al–6% Si alloys after electrorefining experiments in [BMIm]Cl/AlCl$_3$ (40/60 mol%) at +0.6 V for 16.66 h
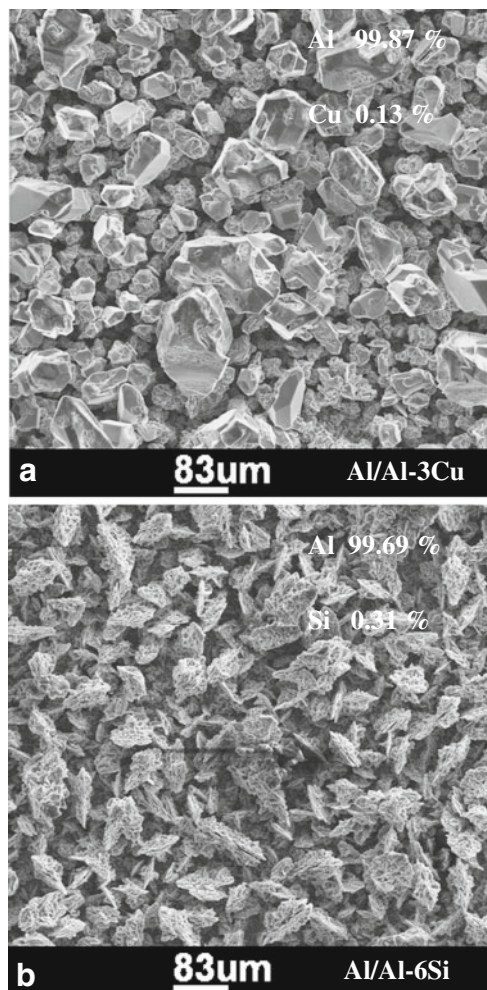

Fig. 9 SEM micrographs of Al-deposits formed on the cathode (Al) during the electrorefining of **a** Al–3%Cu and **b** Al–6% Si alloys at +0.6 V for 16.66 h

of AlCuMgPbFe alloy on gold. The inset of Fig. 7 shows two cyclic voltammograms at two different reversal potentials. As seen, the cyclic voltammogram of Fig. 7 show five cathodic processes with the corresponding anodic counterparts. The first cathodic process (c_1) might be attributable to an under potential deposition process of Cu on Au. The second cathodic wave (c_2) is attributed to the deposition of Cu as a very thin film of Cu was detected on the gold surface after applying a potential of +325 mV. The cathodic peak (c_3) might be attributed to the codeposition of Pb/Fe/Cu. The peak (c_4) recorded before the bulk deposition of aluminum sets in (c_5) might result from alloying of Al with Pb and Cu. Potentiostatic deposition experiments at potentials corresponding to those of peaks (c_3) and (c_4) complemented with SEM–EDX investigations are needed in order to study in more details the nature and composition of the codeposits.

In conclusion, Cu can be solely extracted from the ionic liquid containing the anodic dissolution products of Al–3.7%Cu–0.9%Mg–0.8%Pb–0.6%Fe alloy. Furthermore, after obtaining of all dissolved Cu, Pb/Fe can be codeposited. There is no hint for Mg deposition.

Electrorefining of Al–3%Cu and Al–6%Si alloys

Electrorefining experiments of Al–3%Cu and Al–6%Si alloys were carried out in the ionic liquid [BMIm]Cl/AlCl$_3$ (40/60 mol%) at a constant potential of +0.6 V for 16.66 h. The change in masses of both cathode and anode was determined after experiments. Under the employed experimental conditions, the current efficiencies for both anodic dissolution and aluminum deposition were found to be close to 100%. The energy consumption was about 2 kWh/kg of Al (1.83 and 1.81 kWh/kg for Al–Cu and Al–Si, respectively) which is significantly lower than the energy consumption in the conventional industrial refining process (about 15–18 kWh/kg of Al, [29]).

The surfaces of the alloys after applying an anodic potential of +0.6 V for 16.66 h in the employed ionic liquid were investigated by means of a SEM and by EDX, to explore morphology and composition, respectively (Fig. 8). In general, the examined alloys are subject to anodic dissolution with some hints for galvanic corrosion. The small white particles shown in the SEM micrograph of Fig. 8b are analyzed as Cu revealing the occurrence of galvanic dissolution of Al. Also, the high surface concentration of Si (18.85 wt.%) after anodic oxidation compared with its bulk concentration in the alloy (6%) indicates the occurrence of galvanic corrosion. According to the standard electrode potentials of Al, Cu, and Si, Cu, and Si should be protected cathodically at the expense of aluminum owing to the formation of numerous galvanic sites at the electrode surface.

The deposits obtained on the cathode (pure aluminum) were also investigated (Fig. 9). Generally, the deposits are granular with crystallite sizes in the order of 30–50 μm. The EDX analysis of the deposits on the cathode reveals that the deposits contain low concentrations of the alloying elements. In the case of using Al–3%Cu as an anode, only very low concentration of Cu (0.11 wt.%) is deposited (Fig. 9a). In case of Al–6%Si, the deposits contain 0.31 wt. % Si (Fig. 9b). This signifies that high purity aluminum can be recovered by electrorefining of aluminum alloys in the employed ionic liquids.

Conclusions

The present paper shows the possibility of the extraction of less reactive metals, especially copper, from aluminum alloys in chloroaluminate ionic liquids. The examined alloys were anodically dissolved in the employed ionic liquids and then pure copper was recovered under potentiostatic conditions. Al–6%Si, Al–3%Cu, and Al–3.7%Cu–0.9%Mg–0.8%Pb–0.6%Fe alloys exhibited almost the same anodic behavior in the employed ionic liquids. The alloys were subject to anodic dissolution followed by some sort of passivity. This is attributable to the formation of adsorbed films of the oxidation products on the surface. Electrorefining results show the possibility of recovering of pure aluminum at room temperature with very low energy consumption of about 2 kWh/kg of Al.

References

1. Welch BJ, Osteryoung RA (1981) J Electroanal Chem 118:455–466
2. Zhao Y, VanderNoot TJ (1997) Electrochim Acta 42:1639–1643
3. Moffat TP (1994) J Electrochem Soc 141:L115–L117
4. Ali MR, Nishikata A, Tsuru T (1997) Electrochim Acta 42:2347–2354
5. Stafford GR (1994) J Electrochem Soc 141:945–953
6. Tsuda T, Hussey CL, Stafford GR, Bonevich JE (2003) J Electrochem Soc 150:C234–C243
7. Tsuda T, Hussey CL (2003) J Min Metall B 39:3–22
8. Stafford GR (1989) J Electrochem Soc 136:635–639
9. Moffat TP, Stafford GR, Hall DE (1993) J Electrochem Soc 140:2779–2786
10. Endres F, Bukowski M, Hempelmann R, Natter H (2003) Angewandte Chemie 115:3550, Int. Ed.: (2003) 42:3428–3430

11. Liu QX, Zein El Abedin S, Endres F (2006) Surf Coat Tech 201:1352–1356
12. Jiang T, Brym MJC, Dube G, Lasia A, Brisard GM (2006) Surf Coat Tech 201:1–9
13. Kamavaram V, Mantha D, Reddy RG (2003) J Min Met B 39:43–58
14. Pradhan D, Mantha D, Reddy RG (2009) Electrochim Acta 54:6661–6667
15. Kamavaram V, Mantha D, Reddy RG (2005) Electrochim Acta 50:3286–3295
16. Wilkes JS, Levisky JA, Wilson RA, Hussey CL (1982) Inorg Chem 21:1263–1264
17. Scordilis-Kelly C, Fuller J, Carlin RT, Wilkes JS (1992) J Electrochem Soc 139:694–699
18. Pitner WR, Hussey CL (1997) J Electrochem Soc 144:3095–3103
19. Lipsztajn M, Osteryoung RA (1983) J Electrochem Soc 130:1968–1969
20. Melton TJ, Joyce J, Maloy JT, Boon JA, Wilkes JS (1990) J Electrochem Soc 137:3865–3869
21. Carlin RT, Osteryoung RA (1989) J Electrochem Soc 136:1409–1415
22. Hussey CL (1988) Pure & Appl Chem 60:1763–1772
23. Oye HA, Jagtoyen M, Oksefjell T, Wilkes JS (1991) Mater Sci Forum 73–75:183–190
24. Tierney BJ, Pitner WR, Mitchell JA, Hussey CL, Stafford GR (1998) J Electrochem Soc 145:3110–3116
25. Vaughan J, Dreisinger D (2008) J Electrochem Soc 155:D68–D72
26. Aravinda CL, Mukhopadyay I, Freyland W (2004) Phys Chem Chem Phys 6:5225–5231
27. Endres F, Schweizer A (2000) Phys Chem Chem Phys 2:5455–5462
28. Zell CA, Endres F, Freyland W (1999) Phys Chem Chem Phys 1:697–704
29. Kondo M, Maeda H, Mizuguchi M (1990) JOM 42:36–37